Kinetic analysis of the RNA cleavage of the conformationally-constrained oxetane-modified antisense-RNA hybrid duplex by RNase H †

Nariman V. Amirkhanov, Pushpangadan I. Pradeepkumar and Jyoti Chattopadhyaya *

Department of Bioorganic Chemistry, Biomedical Center, University of Uppsala, Box 581, S-75123 Uppsala, Sweden. E-mail: jyoti@bioorgchem.uu.se; Fax: +4618-554495; Tel: +4618-4714577

Received (in Cambridge, UK) 14th December 2001, Accepted 26th February 2002
First published as an Advance Article on the web 20th March 2002

The kinetics of the complementary 15mer RNA (**3**) cleavage by RNase H in the conformationally-constrained [North-East type sugar constraint] triple oxetane modified antisense oligonucleotide AON (**2**)–RNA (**3**) hybrid duplexes (P. I. Pradeepkumar and J. Chattopadhyaya, *J. Chem. Soc., Perkin Trans. 2*, 2001, 2074) have been investigated, in comparison with the native 15mer counterpart AON (**1**)–RNA (**3**), by changing both AON and RNA concentrations, while keeping the enzyme and buffer concentrations constant. The RNA concentration-dependent kinetics of the RNase H promoted cleavage reaction gave values for K_m and V_{max} for both substrates: AON (**1**)–RNA (**3**) and AON (**2**)–RNA (**3**) heteroduplexes. The V_{max} and the K_m values were respectively ~2 and ~10 times greater for the AON (**2**)–RNA (**3**) duplex than those for the native counterpart, which means that the incorporation of the North-East type sugar constrained triple oxetane modifications in the AON increases the catalytic activity of RNase H by almost *ca.* 2-fold owing to the decreased affinity of the substrate toward the enzyme. The T_m for the AON (**2**)–RNA (**3**) hybrid duplex was 18 °C less than that of the native. Thus, an inverse correlation between AON–RNA hybrid duplex thermostability and RNase H activity has been found under the high substrate concentration conditions. Under high substrate concentration conditions, the RNase H activity of the AON (**2**)–RNA (**3**) hybrid duplex is however higher than the native because of a more rapid turn over (N_{max}) of RNase H. Conversely, under low substrate concentration conditions, the RNase H activity of AON (**2**)–RNA (**3**) hybrid duplex dramatically drops compared to the native because of the less effective turn over (N_{eff}) of enzyme. This is because the N_{eff}, under low substrate concentration conditions, depends on maximal turn over, N_{max}, as well as on the extent of saturation of enzyme by substrate, which in turn depends upon the value of the V_{max}/K_m ratio, which for the AON (**2**)–RNA (**3**) hybrid duplex has been found to be ~4-fold less than the native.

Introduction

Antisense oligonucleotides (AON) (Fig. 1) such as boranophosphates,[1,2] phosphorothioates[1–5] and chimeric methylphosphonate/phosphodiesters,[7–9] show a higher initial velocity of RNA cleavage by RNase H[6] at a high substrate (*i.e.* AON–RNA hybrid duplex) concentration (10–1000 μM),[1–5,7–9] compared with those of the native.[1–5,7–10] For AONs based on boranosphosphates,[1,2] phosphorothioate[1–5] and chimeric methylphosphonate/phosphodiesters,[7–9] it has been shown that the RNase H activity is inversely proportional to the thermal stability of the substrate under conditions of substrate saturation for the enzyme. Studies on the concentration dependent affinity (K_m) of the substrate toward RNase H have been performed for phosphorothioates[11,12] as well as for various gapmers based on 2′-modifications[11,13*a*,14] but no such study has been so far made for boranophosphates[1,2] and chimeric methylphosphonate/phosphodiesters.[7–9] At the enzyme saturation condition by the substrate, only V_{max} or k_{cat} should control the initial rates of RNase H cleavage activity, not K_m. When the enzyme is not saturated by the substrate under a low substrate concentration (*i.e.* when the substrate concentration is less than K_m), the affinity of the substrate toward the enzyme may however dictate the initial velocity according to the Michaelis–Menten equation. Thus a knowledge of initial velocity at different substrate concentrations for the RNA cleavage by RNase H is important to understand how the RNase H actually works towards different substrates under

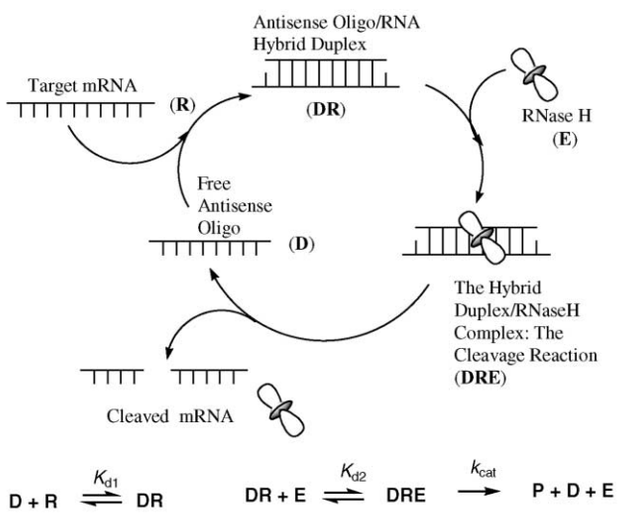

Fig. 1 The catalytic RNase H promoted cleavage of the target mRNA through the formation of antisense oligonucleotide–RNA hybrid duplex. The kinetic scheme of the RNase H hydrolysis is shown in the bottom part of the cartoon, where D is AON (antisense oligo); R is the target RNA; K_{d1} is the equilibrium constant of dissociation of the heteroduplex DR; K_{d2} is equilibrium constant of dissociation of the substrate–enzyme complex DRE.

† Electronic supplementary information (ESI) available: autoradiograms of denaturing PAGE gels. See http://www.rsc.org/suppdata/p2/b1/b111438g/

 DOI: 10.1039/b111438g

different conditions. This will enable us to predict eventually how a potentially successful AON would behave in cellular conditions, which will, in turn, help to improve the design of a potentially successful AON.

The initial velocity or extent of cleavage of the RNase H promoted cleavage of the RNA strand in the AON–RNA duplex (Fig. 1) depends on one kinetic (k_{cat}) and two thermodynamic (K_{d1} and K_{d2}) parameters. This means that the cleavage activity by RNase H can change in a different manner under different conditions depending on specific AON–RNA systems. In order to obtain detailed understanding of the substrate properties of different AONs in hybrid AON–RNA duplexes toward RNase H, kinetic experiments should be performed both by changing the RNA and the AON concentration.[15] Simple, two-step enzymatic reactions can be analyzed by the well known Michaelis–Menten mechanism.[16,17] It is however difficult to use this approach to RNase H promoted reactions, where we have an additional step for the formation of AON–RNA duplexes (K_{d1}; Fig. 1), because we do not actually know the real substrate concentration in the system. It is very important to take K_{d1} into account in case of poorly thermostable duplexes, and in those cases, the substrate (duplex) concentration can be very far from the real RNA concentration. Clearly, the first step of this 3-step process can be circumvented by performing the Michaelis–Menten kinetics under RNA saturation conditions.[15]

Several RNase H affinity studies have been performed so far to aid understanding of the substrate specificity, preference and tolerance for modifications in the antisense DNA strand of the hybrid duplex.[10–14] It has emerged that the RNA in the various hybrid duplexes containing 2′-modified chimeric AONs (*e.g.* 2′-F, -OMe, -OPr, -OCH_2CH_2OMe *etc.*) was digested by RNase H *ca.* 3-fold more slowly than the wild type duplexes.[14] It has been recently shown from various laboratories that incorporation of 3′-*endo* (North-type) sugar conformation constrained[18–21] nucleotide preorganizes the AON strand into an A-RNA type conformation, because of combined forces of both stereoelectronic gauche and anomeric effects,[22,23] inducing the heteroduplex conformation into an RNA–RNA type duplex. This conformational mimicry by the AON–RNA heteroduplex enhances its stability,[18–21] but that often results into a much reduced catalytic RNase H promoted cleavage of the RNA strand in the heteroduplex.[19,20]

The North-East constrained 1-(1′,3′-*O*-anhydro-β-D-psicofuranosyl)thymine[21] (the oxetane) have unique conformational features in that the phase angle (P) and the puckering amplitude (ϕ_m) of the constrained pentofuranose moiety with *anti*-aglycone varies from 42° < P < 45° and 22° < ϕ_m < 29° (B3LYP/6-31G* gas phase, Gaussian 96).[23] The introduction of up to three oxetane modifications in the AON strand, as in **2**, results in reduction of T_m by ~18 °C (~6 °C per modification)[21] without any concomitant loss of RNase H cleavage of the complementary RNA, compared to the wild type heteroduplex[21c] (Fig. 2) under RNA saturation conditions. This characteristic behavior of the oxetane-modified AON–RNA duplex toward RNase H and the cleavage reaction has prompted us to examine the nature of RNase H recruitment, substrate recognition, specificity and cleavage[14,18,20] *vis-à-vis* conformational preorganization in the AON–RNA heteroduplexes by the AON.

We here report a detailed kinetic study of the RNA (**3**) cleavage by RNase H of these North-East type conformationally-constrained triple oxetane modified antisense oligonucleotide AON (**2**)–RNA (**3**) hybrid duplexes[21] and compare with those of the native 15mer counterpart AON (**1**)–RNA (**3**) hybrid.

Results

The extent of RNA cleavage by RNase H in all AON (**1**, **2**)–RNA (**3**) duplexes were investigated both (i) by changing the AON concentration (Figs. 3–5), at a constant concentration of

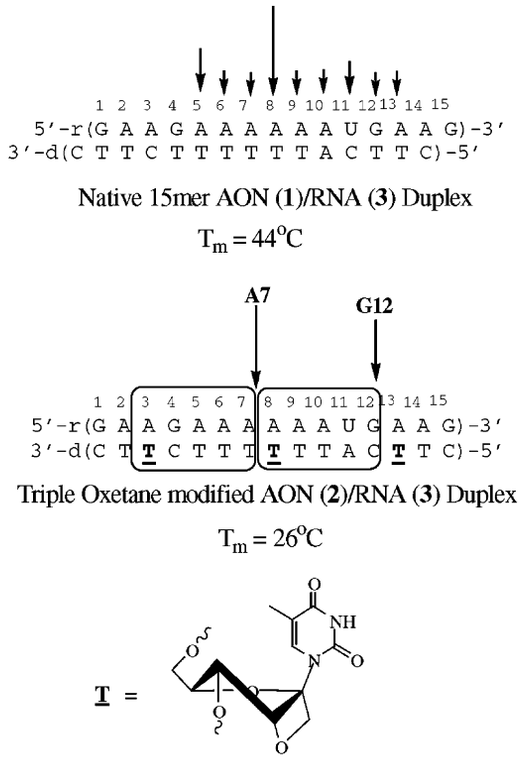

Fig. 2 Structures of the hybrid duplexes of the native 15mer AON (**1**) and triple oxetane-modified AON (**2**) with the target RNA (**3**). Note that the thermodynamic stability of the hybrid duplex **2** + **3** is 18 °C lower than the native counterpart. The vertical arrows show the RNA cleavage sites, and the relative length of an arrow shows the relative extent of cleavage at that site (see Fig. 3 for the PAGE pictures, and supplementary information for detailed PAGE for kinetic measurements). It is also noteworthy that the native **1** + **3** duplex has virtually no preference for complementary RNA cleavage by RNase H, whereas the oxetane-modified **1** + **3** duplex cleaves mainly at A7 and G12 (see text).

RNA and RNase H in order to obtain saturation conditions for RNA (*i.e.* when RNA is completely bound to the AON in the hybrid duplex form) in the presence of an excess of AON, and also (ii) by changing the RNA concentration (Figs. 3, 6–8) at a constant concentration of RNase H and AON, which is sufficient for complete saturation of RNA (see supplementary information on PAGE).

The summary of our investigation is as follows.

(1) The initial velocities (v_0) have been obtained at five different AON concentrations (ranging from 0.01 to 1 μM) (Figs. 3–5), which were subsequently plotted as a function of AON concentration, to give the equilibrium constant of the dissociation (K_{d1}) for the hybrid AON (**2**)–RNA (**3**) duplex.

(2) The extent of the target RNA cleavage by RNase H in the hybrid AON (**2**)–RNA (**3**) duplex at saturation conditions (when RNA is completely saturated by AON at low RNA concentration) is lower than in the native 15mer AON (**1**)–RNA (**3**) duplex (Figs. 3–5). The data thus show a good correlation of the initial velocity of RNase H activity with the thermostability of the corresponding hybrid AON (**2**)–RNA (**3**) (T_m = 26 °C) and AON (**1**)–RNA (**3**) (T_m = 44 °C) duplexes.

(3) When the AON concentration for **1** or **2** is increased, we see an increase of the extent of cleavage along with the increase of the height of the saturation plateau (Fig. 5). The plot of this AON concentration-dependent study is hyperbolic in nature, which appears sigmoidal in shape in the logarithmic scale as shown in Fig. 5B. The AON concentration at the inflection point of the plot (Fig. 5B) of the AON concentration dependent RNA cleavage rate gives the equilibrium constant of the dissociation (K_{d1}) for the hybrid AON (**2**)–RNA (**3**) duplex, which is 0.16 μM. It is noteworthy that it is not possible to get

Table 1 Dependence of the initial velocity (v_0[a]) on the substrate concentration

	$v_0/10^{-2}$ μM min^{-1}	
S_0 ([RNA]/μM)	Native 15mer-AON (**1**)	Triple oxetane modified AON (**2**)
0.04	0.741	0.328
0.06	0.838	0.328
0.08	1.320	0.581
0.1	1.269	0.774
0.2	1.378	1.151
0.4	1.942	1.797
0.6	1.580	1.992
1	1.755	2.816

[a] Initial velocity (v_0) has been calculated from the data taken up to 5 min of the reaction (see Figs. 3, 6 and 7, and supplementary information for kinetics based on PAGE).

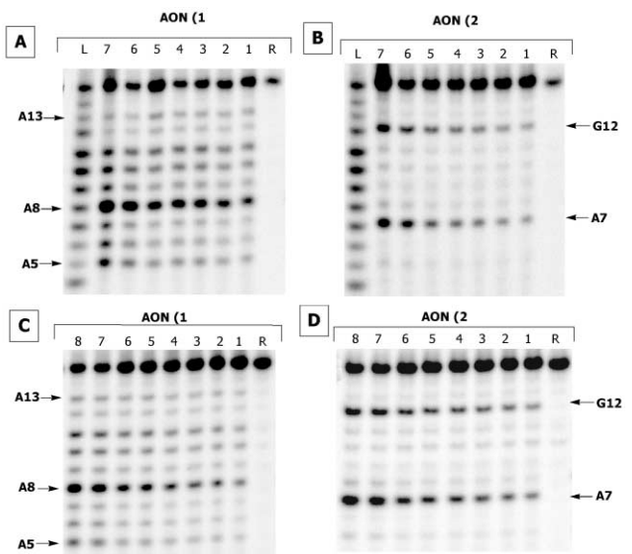

Fig. 3 Autoradiograms of the 20% denaturing PAGE, showing kinetics of the complementary 5′-^{32}P-labelled target RNA (**3**) cleavage by RNase H in the native 15mer AON (**1**)–RNA (**3**) [gels **A** and **C**] and oxetane-AON (**2**)–RNA (**3**) [gels **B** and **D**] hybrid duplexes. Lane R: ^{32}P-labelled target RNA (**3**) without AON; lane L: snake venom PDE ladder. Lanes 1–7 (in **A** and **B**): aliquots of the digest taken after 2, 4, 6, 7, 8, 10 and 90 min, respectively. Lanes 1–8 (in **C** and **D**): aliquots of the digest taken after 2, 3, 4, 5, 6, 7, 20 and 90 min respectively. Conditions of cleavage reaction: AON (0.05 μM in **A** and **B**, 5 μM in **C** and **D**) and RNA (0.01 μM in **A** and **B**, 0.2 μM in **C** and **D**) in buffer, containing 20 mM tris–HCl (pH 8.0), 20 mM KCl, 10 mM $MgCl_2$, 0.1 mM EDTA and 0.1 mM dithiothreitol (DTT), 21 °C, 0.06 U of RNase H. Total reaction volume is 30 μl (see supplementary information for a detailed kinetic picture by PAGE).

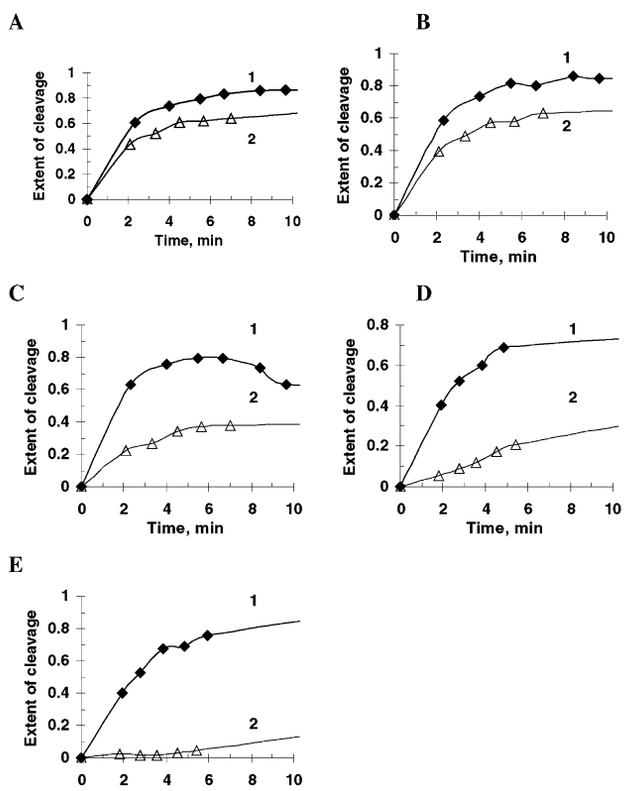

Fig. 4 Extent of hydrolysis of the 15mer target RNA (0.01 μM) in the AON–RNA hybrid duplexes by RNase H as a function of the reaction time. Curves 1 and 2 in **A** to **E** correspond to the hybrid duplexes formed by native 15mer AON (**1**) and triple oxetane modified AON (**2**), respectively, with the complementary RNA (**3**). *Conditions of the cleavage reactions*: AON concentration at 1 μM in **A**, 0.5 μM in **B**, 0.1 μM in **C**, 0.05 μM in **D** and 0.01 μM in **E**, with constant RNA (**3**) concentration at 0.01 μM in buffer, containing 20mM tris–HCl (pH 8.0); 20 mM KCl, 10 mM $MgCl_2$. 0.1 mM EDTA and 0.1 mM dithiothreitol (DTT), 21 °C, 0.06 U of RNase H. Total reaction volume is 30 μl.

the exact K_{d1} value for the native counterpart under the present measurement conditions, since we are limited by RNA concentration (0.01 μM) *vis-à-vis* AON and RNase H concentration (AON concentration should be more than the RNA concentration in order to get correct K_{d1}).

(4) The initial velocities (v_0) have also been obtained at eight different RNA concentrations (ranging from 0.04 to 1 μM) (Figs 3, 6, 7 and Table 1) at saturating conditions for RNA (**3**) by AON (**1**, **2**) (5 μM), which were subsequently plotted as a function of substrate, RNA–AON hybrid duplex, concentration (S_0) (Fig. 7) to give the K_m, V_{max} and k_{cat} by the Michaelis–Menten equation,[16] as described by $v_0 = V_{max} \times [S_0]/(K_m + [S_0])$ (Figs. 3C, 3D, 6, 7, Tables 1–3).

(5) Since $V_{max} = E_0 k_{cat}$ (E_0 = initial enzyme concentration), and for all of our RNA concentration dependent kinetics, the E_0 value was identical, hence V_{max} is proportional to k_{cat}. This shows that the relative k_{cat} can be understood by comparing simply the V_{max}. Table 3 thus shows V_{max}/K_m or k_{cat}/K_m for all AONs in the corresponding AON–RNA duplexes, showing the enzyme affinity of the heteroduplex in comparison with the native counterpart. Comparison of values of V_{max}/K_m is important since V_{max} and K_m would be expected to change in a compensating manner at a fixed E_0.[13a,16,17] Thus, the V_{max}/K_m value for AON (**2**)–RNA is 5-fold less than the native counterpart (Table 3).

(6) For triple oxetane-modified AON (**2**), the cleavage sites have been found to be at mainly A7 and G12 positions (Figs. 2 and 3) of the complementary target RNA compared to that of the native 15mer AON (**1**), which had a main cleavage site at A8 and minor cleavage sites from A5 to A13 positions (Figs. 2 and 3). The 5-nucleotide long footprint found[21] in the RNase H cleavage reaction (Figs. 2 and 3) in the triple oxetane-modified AON (**2**)–RNA (**3**) is owing to the fact that it takes up an

RNA–RNA type conformation, which is resistant to cleavage by RNase H. This is a case of conformational transmission of the constrained 3′-*endo* sugar of the oxetane **T** nucleotide to the neighboring nucleotides, which is transmitted up to a stretch of 5 nucleotides in the heteroduplex. Interestingly, the junction A7, lying between two 5-nucleotide long stretches, is cleaved preferentially over G12 (at the end of the T8 box shown in Fig. 2) by RNase H because it probably takes up a sugar–phosphate backbone conformation more akin to the DNA–RNA type conformation. The additional, but minor, A8 RNA cleavage site appearing at *low* RNA concentration (*i.e.* at low substrate concentration; shown in Fig. 3S: (A) and (B) in supplementary information) compared to the high RNA

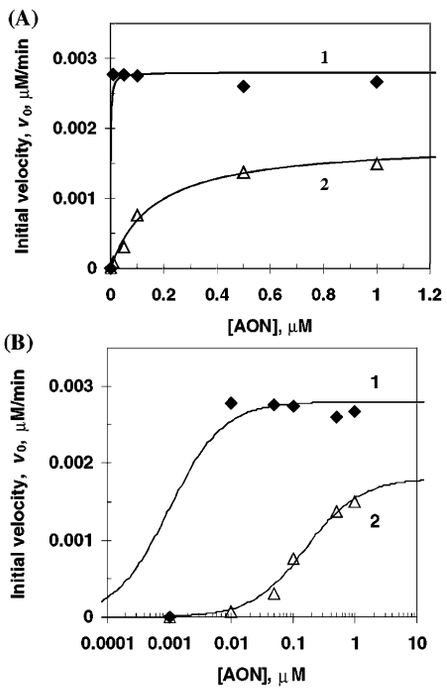

Fig. 5 Initial velocity of the hydrolysis of the 15mer target RNA (0.01 μM) in the AON–RNA hybrid duplexes by RNase H as a function of the AON concentration (the concentrations of AONs range from 0.01, 0.05, 0.1, 0.5 and 1 μM. Curves 1 and 2 in **A** and **B** correspond to the hybrid duplexes formed by native 15mer AON (**1**) and oxetane modified AON (**2**) respectively. *Conditions of the cleavage reactions*: AON concentration at 0.01–1 μM with constant RNA (**3**) concentration at 0.01 μM in buffer, containing 20 mM tris–HCl (pH 8.0), 20 mM KCl, 10 mM $MgCl_2$, 0.1 mM EDTA and 0.1 mM dithiothreitol (DTT), 21 °C, 0.06 units of RNase H. Total reaction volume is 30 μl. (**A**) Normal hyperbolic plots. (**B**) Logarithmic scale of S_0 concentration (sigmoidal plots). Equilibrium constants of the dissociation for the duplex AON (**1**)–RNA (**3**), $K_{d1} < 0.01$ μM, and for duplex AON (**2**)–RNA (**3**), $K_{d1} = 0.16$ μM, mean that K_{d1} for the duplex AON (**1**)–RNA (**3**) is more than 16 times less than K_{d1} for the duplex AON (**2**)–RNA (**3**). This means that AON (**1**)–RNA (**3**) heteroduplex is more than 16 times more thermostable compared to AON (**2**)–RNA (**3**).

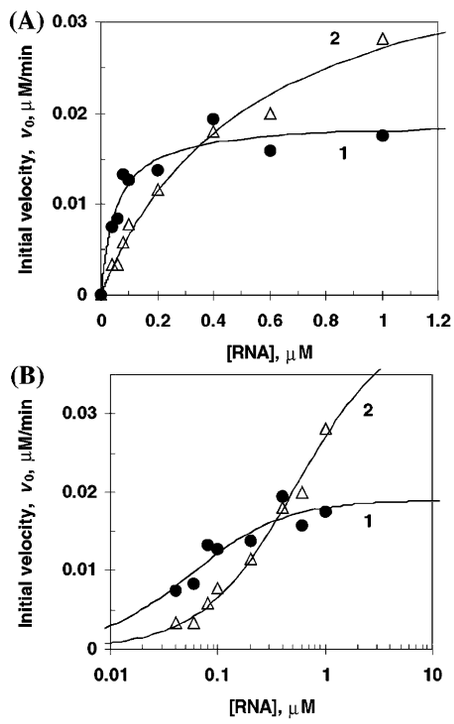

Fig. 7 Initial velocity of the hydrolysis of the 15mer target RNA (**3**) in the AON–RNA hybrids by RNase H as a function of the RNA concentration (the concentrations of RNA range from 4×10^{-8} to 10^{-6} M). Curves 1 and 2 correspond to the hybrid duplexes formed by native 15mer AON (**1**) and oxetane modified AON (**2**) respectively. Conditions of cleavage reaction: AON (**1** or **2**) (5 μM) and RNA (**3**) in buffer, containing 20 mM tris–HCl (pH 8.0), 20 mM KCl, 10 mM $MgCl_2$, 0.1 mM EDTA and 0.1 mM dithiothreitol (DTT), 21 °C, 0.06 units of RNase H. Total reaction volume is 30 μl. (**A**) Normal hyperbolic plots. (**B**) Logarithmic scale of S_0 concentration (sigmoidal plots).

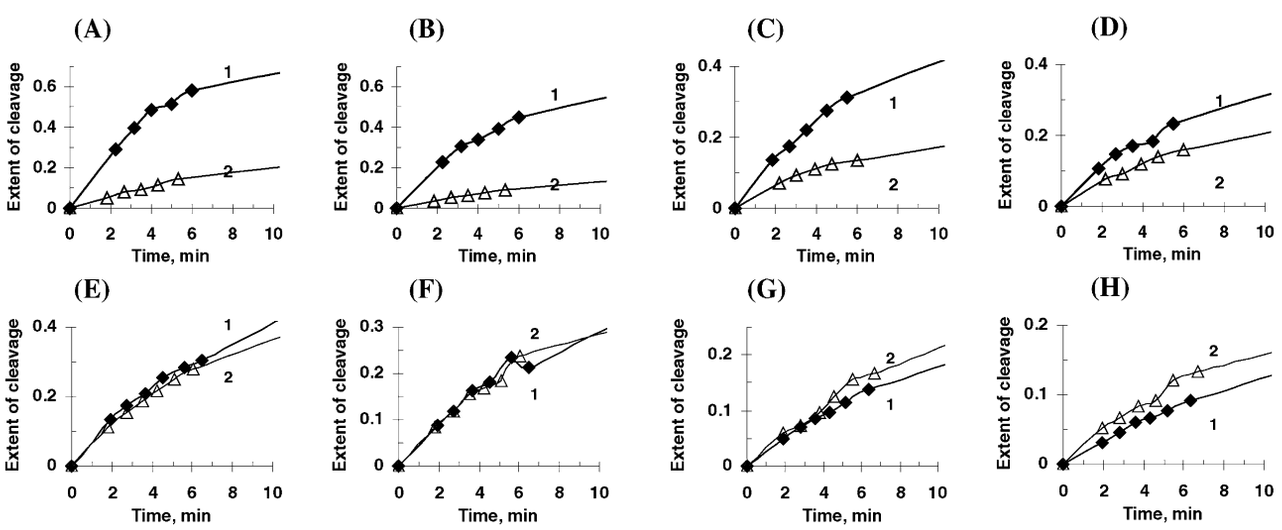

Fig. 6 Extent of hydrolysis of the target RNA (**3**) in the AON–RNA hybrids by RNase H as a function of the reaction time. Curves 1 and 2 in **A** to **H** correspond to the hybrid duplexes formed by native 15mer AON (**1**), and oxetane modified-AON (**2**) respectively. *Conditions of the cleavage reactions*: AON concentration (5 μM) and RNA (**3**) were varied at 0.04 μM in **A**, 0.06 μM in **B**, 0.08 μM in **C**, 0.1 μM in **D**, 0.2 μM in **E**, 0.4 μM in **F**, 0.6 μM in **G** and 1 μM in **H** in buffer, containing 20 mM tris–HCl (pH 8.0), 20 mM KCl, 10 mM $MgCl_2$, 0.1 mM EDTA and 0.1 mM dithiothreitol (DTT), 21 °C, 0.06 units of RNase H. Total reaction volume is 30 μl.

Table 2 Dependence of the extent of cleavage (P/S_0) of RNA on the substrate (*i.e.* hybrid duplex) concentration

	$\alpha = \Delta P/S_0 = v_0 \times t$ [a]	
S_0 ([RNA]/μM)	Native 15mer-AON (**1**)	Triple oxetane modified AON (**2**)
0.04	0.74	0.33
0.06	0.56	0.22
0.08	0.66	0.29
0.1	0.51	0.31
0.2	0.28	0.23
0.4	0.19	0.18
0.6	0.11	0.13
1	0.07	0.11

[a] Extent of cleavage has been calculated from the data taken during $t = 4$ min of the reaction (see Fig 8).

Table 3 Kinetic characteristics[a] of RNA cleavage by RNase H in the hybrid duplex

Substrate	V_{max}/μM min^{-1}	K_m/μM	k_{cat}/min^{-1}	(V_{max}/K_m)/min^{-1}	(k_{cat}/K_m)/min^{-1} μM^{-1}	Relative k_{cat}/K_m
15mer-AON (**1**) + RNA (**3**)	0.0190 ± 0.0053	0.0551 ± 0.015	83.8 ± 23.4	0.3448	1521	1
Oxetane modified AON (**2**) + RNA (**3**)	0.0415 ± 0.0035	0.5347 ± 0.045	183.0 ± 15.4	0.0776	342.3	0.225

[a] $V_{max} = k_{cat}E_0$ ($E_0 = 0.06$ units/30 μl $= 2 \times 10^{-3}$ units μl$^{-1} = 2.26757 \times 10^{-4}$ μM), specific activity = 420000 units mg$^{-1} = 1.13386 \times 10^{-13}$ moles per unit, MW = 21000 grams per mole.

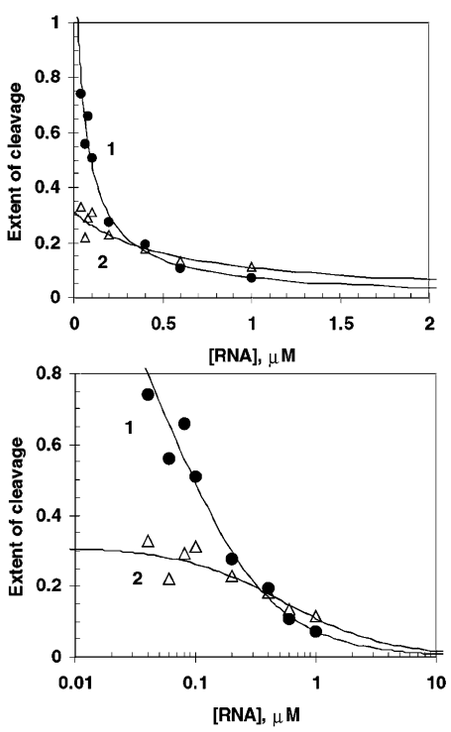

Fig. 8 Extent of cleavage ($\Delta P/S_0$, where P is the amount of cleavage product formed and S_0 is the initial concentration of the substrate (*i. e.* hybrid duplex) of the 15mer target RNA (**3**) in the AON–RNA hybrids by RNase H as a function of the RNA concentration (the concentrations of RNA range from 4×10^{-8} to 10^{-6} M): **A** shows normal hyperbolic plots, and **B** is in the logarithmic scale, giving sigmoidal plots of S_0 concentration. Curves 1 and 2 correspond to the hybrid duplexes formed by native 15mer AON (**1**) and oxetane modified AON (**2**) respectively. They show that under the saturation conditions of RNA by AON, the extent of the cleavage reaction of the complementary RNA by RNase H slows down as the concentration of RNA goes up. Conditions of cleavage reaction: AON (**1** or **2**) (5 μM) and RNA (**3**) in buffer, containing 20 mM tris–HCl (pH 8.0), 20 mM KCl, 10 mM $MgCl_2$, 0.1 mM EDTA and 0.1 mM dithiothreitol (DTT), 21 °C, 0.06 units of RNase H. Total reaction volume is 30 μl.

concentration studies (*i.e.* Fig. 3S: (E)–(H) in supplementary information) shows that the affinity of the enzyme for the A8 site is more than those of A7 and G12 sites. The extent of cleavage at the A8 site however becomes negligible compared to A7 and G12 cleavage sites. This is because at *high* substrate concentration the enzyme affinity for A8 plays a very minor role and only the V_{max} or k_{cat} dictates the turnover of the reaction.

Discussion

The dependence of the initial velocity, v_0, of the cleavage reaction on the substrate concentration (S_0 = [RNA]) has been interpreted (Figs. 3C, 3D, 6 and 7, and Table 1) according to the Michaelis–Menten equation, eqn. (1)[16] (see methods in the Materials and methods section), where v_0 in the enzyme unsaturated conditions (when $S_0 \leq K_m$) increases with the increase of S_0, and has a saturation plateau when $S_0 \longrightarrow \infty$ (Fig. 7). Thus, the native 15mer (**1**) has more cleavage activity than that of the oxetane modified AON (**2**) in the area where $S_0 < 0.1$ μM, and the relative activity switches in the opposite direction in the area where $S_0 > 1$ μM (Fig. 7 and Table 1).

Under *low substrate concentration*, when $S_0 \ll K_m$ (see eqn. (2) in the Materials and methods section), v_0 is linearly dependent upon the substrate concentration (Fig. 7A, see area $S_0 < 0.2$ μM) with the linear coefficient of V_{max}/K_m, which is more for the heteroduplex formed with the native 15mer-AON (**1**) and less for the duplex formed with the triple oxetane-modified AON (**2**) (Table 3).

Under *high substrate concentration*, when $S_0 \gg K_m$ (see eqn. (3)), v_0 is dependent only on V_{max} or, alternatively, on k_{cat} and E_0. The plot of v_0 as a function of RNA concentration in Fig. 7 shows that v_0 has a maximal value at V_{max} under saturation conditions. V_{max} for the triple oxetane modified AON hybrid duplex **2** + **3** is ~2 times larger than that for the hybrid duplex **1** + **3** (Table 3), which shows that the oxetane modified substituent in the former indeed enhances the catalytic activity of RNase H (Fig. 7, when $S_0 > 0.4$ μM).

It is noteworthy that although there is an increase in the initial velocity of RNA cleavage by RNase H for both hybrid duplexes, the extent of the cleavage ($\alpha = \Delta P/S_0$) decreases (eqn. (4)) inversely with an increase of substrate concentration (S_0 = [RNA]) (Fig. 8, Table 2)

The effective turn over (N_{eff}) of RNase H per min has been calculated by using eqn. (6). The effective turnover of the enzyme depends on factors such as the k_{cat} and F_e (eqn. (6a)); F_e

Table 4 Turnovers[a] (N_{eff} and N_{max}), extent of cleavage[a] and extent of saturation of enzyme by AON–RNA substrates, F_e, for RNase H cleavage reactions in different substrate concentrations, S_0

Substrate, S_0	S_0 ([RNA]/μM)	$F_e = [ES]/S_0 = S_0/(K_m + S_0)$	N_{max} ($V_{max}/E_0 = k_{cat}$)/min^{-1}	N_{eff} ($F_e N_{max}$/min^{-1})	Extent of cleavage/min^{-1}	$N_{relative}$ (N_{eff}(AON)/N_{eff} (15mer)
15mer-AON (**1**) + RNA (**3**)	0.04	0.421	83.8	35.24	0.200	1
Oxetane modified AON (**2**) + RNA (**3**)	0.04	0.070	183.0	12.74	0.072	0.36
15mer-AON (**1**) + RNA (**3**)	0.06	0.521	83.8	43.68	0.165	1
Oxetane modified AON (**2**) + RNA (**3**)	0.06	0.101	183.0	18.46	0.070	0.42
15mer-AON (**1**) + RNA (**3**)	0.08	0.592	83.8	49.62	0.141	1
Oxetane modified AON (**2**) + RNA (**3**)	0.08	0.130	183.0	23.82	0.068	0.48
15mer-AON (**1**) + RNA (**3**)	0.1	0.645	83.8	54.02	0.123	1
Oxetane modified AON (**2**) + RNA (**3**)	0.1	0.158	183.0	28.83	0.065	0.53
15mer-AON (**1**) + RNA (**3**)	0.2	0.784	83.8	65.69	0.074	1
Oxetane modified AON (**2**) + RNA (**3**)	0.2	0.272	183.0	49.82	0.0564	0.76
15mer-AON (**1**) + RNA (**3**)	0.4	0.879	83.8	73.65	0.042	1
Oxetane modified AON (**2**) + RNA (**3**)	0.4	0.428	183.0	78.32	0.044	1.06
15mer-AON (**1**) + RNA (**3**)	0.6	0.916	83.8	76.74	0.029	1
Oxetane modified AON (**2**) + RNA (**3**)	0.6	0.529	183.0	96.77	0.037	1.26
15mer-AON (**1**) + RNA (**3**)	1	0.948	83.8	79.41	0.018	1
Oxetane modified AON (**2**) + RNA (**3**)	1	0.652	183.0	119.3	0.027	1.50

[a] N_{max}; N_{eff} and extent of cleavage during one min of the reaction. N_{max} is maximal turnover of enzyme per min, when the enzyme is 100% saturated with the substrate. The effective turn over (N_{eff}) of RNase H in 1 min has been calculated by eqn. (6), see Materials and methods section. N_{eff} indicates the number of RNA molecules the enzyme cleaves per min; F_e is the extent of saturation of enzyme (see eqn. (6a) in the Materials and methods section). N_{max} is the maximal turn over of enzyme per min, when the extent of saturation of the enzyme by substrate is maximal, otherwise $F_e = 1$ (see eqn. (7) in the Materials and methods section).

is also dependent on both K_m and S_0. It means that under different substrate concentration, S_0, the effective turnover of enzyme, N_{eff}, will be different. We have therefore calculated the values for N_{eff} for each AON at different substrate concentrations (Table 4). The data show that the N_{eff} value of RNase H for native 15mer-AON–RNA is 35.2 min^{-1} at *low RNA concentration* ([S_0] = 0.04 μM) compared to that of triple-oxetane modified AON (N_{eff} = 12.7 min^{-1}). This is because the native substrate under these conditions saturates the RNase H more (F_e = 0.42 or 42%) compared to the oxetane substrate (F_e = 0.07 or 7%). On the other hand, at a *high RNA concentration* ([S_0] = 1 μM), the N_{eff} value for **2** + **3** is 119.3 min^{-1} compared to that of the native (N_{eff} = 79.4 min^{-1}) (Table 4) because the enzyme saturation (F_e) is 94% for the native while it is 65% for the oxetane modified substrate. Thus the ratio of F_e *vis-à-vis* N_{max} drives N_{eff} (Table 4).

The data for v_0, α and N_{eff} were obtained using a large excess (5 μM) of AONs (Figs. 3C, 3D, 6–8, Table 4). Clearly, under such a large excess of AON, the performance of the triple oxetane modified AON, compared to the native, depends entirely only upon the substrate concentration, which is exactly dictated by RNA concentration (Fig. 5). It is noteworthy that under these conditions, the extent of saturation of RNA (F_{RNA}) (eqn. (8)) with AON reach *ca.* 100%. Thus Figs. 4E and 5 clearly show that at [AON] = *0.01 μM*, the native form has *ca.* 100% duplex but the triple-oxetane modified AON has less than 10% of the hybrid duplex.

The initial velocity of the RNA cleavage reaction in constant RNA concentration (eqn. (9)) should depend upon both the V_{max}/K_m ratio and the thermostability of the AON–RNA duplex (F_{RNA}), which are much better for native 15mer-AON (**1**) compared with triple oxetane modified AON (**2**). This might explain why we have a greater initial velocity for RNA cleavage for the more thermostable 15mer-AON, compared to the less thermostable triple oxetane modified AON (Figs. 4E and 5) at the low (0.01 μM) concentration of AON.

In saturated conditions, when [AON] = $D_0 \gg K_{d1}$ ((eqn. (8)), *i.e.* RNA is saturated by AON, the initial velocity is maximal, which is dependent only upon V_{max}/K_m and initial RNA concentration (R_0) (*i.e.* only on the value of V^D_{max} (eqn. (11)), and not on the AON concentration because in this case F_{RNA} = 1 (see eqn. (8)). Clearly, under the same RNA concentration, the value for V^D_{max} is more for 15mer-AON (**1**) compared to triple oxetane modified AON (**2**). This explains why we have different saturation plateaus for different AONs in the AON concentration dependent plots, as shown in Figs. 4 and 5.

Conclusion

(1) The oxetane modifications lead to a less stable duplex, which has a higher K_m and V_{max}. Owing to this reason, at substrate concentrations below K_m, the native AON (**1**)–RNA (**3**) substrate is cleaved more rapidly. At saturating substrate conditions, however, the triple oxetane modified AON (**2**)–RNA (**3**) duplex is cleaved faster than the native because of the higher k_{cat} for the former.

(2) Earlier literature procedures for determining the kinetic behavior of AON–RNA duplexes toward RNase H was entirely based on the Michaelis–Menten mechanism because all heteroduplexes in question had very high thermodynamic stability. This means that the extent of duplex formation was 100% under the kinetic measurement conditions, *i.e.* substrate concentration was equal to RNA concentration.[10,12–14] The thermodynamic stability of our oxetane based AON–RNA duplexes strongly influence the efficiency of the kinetics of the RNA cleavage by RNase H. It has been thus found that the less thermostable duplex gives a greater K_m (less affinity to the enzyme) and a greater V_{max}.

(3) The novelty of the oxetane modified AONs over other modified AONs is that it has a natural phosphate backbone, hence no non-specific binding to protein is expected, as found with some phosphorothioates.[24] It is 4–5 times more endonuclease resistant compared to the native form, thus it has a longer life-time in the cellular media when the 3′-exonucleolytic activity is also arrested by an appropriate 3′-substituent (such as 3′-dipyridophenazine group).[21c]

(4) Earlier, it was qualitatively shown[25] that a high affinity locked nucleic acid analog based AONs were capable of activating RNase H. This is however the first quantitative report where it is clearly demonstrated that the locked nucleic acids such as oxetane modified AONs can indeed recruit RNase H efficiently; of course the efficiency of the cleavage reaction is entirely controlled by the available RNA concentration in the system. Thus the oxetane modified AON is a relatively slow RNase H recruiting agent in the low RNA concentration domain (~0.1 μM), whereas its capability to recruit RNase H is as good as the native counterpart at a higher RNA concentration regime (>0.2 μM), relative to AON concentration (~5 μM).

Materials and methods

Materials

T4 polynucleotide kinase (30 units μL^{-1}) and *E. coli* RNase H (5 units μL^{-1}, specific activity 420000 units mg^{-1}, molecular weight 21000 g mol^{-1}) and [γ-^{32}P]ATP were purchased from Amersham Pharmacia Biotech (Sweden), phosphodiesterase I from *Crotalus Adamanteus* venon was from SIGMA. Oligonucleotides (**1**) and (**2**) and RNA (**3**) were synthesized using an Applied Biosystems 392 automated DNA–RNA synthesizer. Synthesis of the oxetane modified AON (**2**) was carried out as previously described.[21]

UV melting experiments

Determination of the T_ms of the AON–RNA hybrid duplexes was carried out in a buffer, containing 20 mM tris–HCl (pH 8), 100 mM KCl and 10 mM $MgCl_2$. Absorbance was monitored at 260 nm in the temperature range from 3 to 70 °C using a Lambda 40 UV spectrophotometer equipped with Peltier temperature programmer with the heating rate of 1 °C per minute. Prior to the measurements samples (1 : 1 mixture of 1 µl AON and 1 µl RNA) were preannealed by heating to 80 °C for 5 min followed by slow cooling until 3 °C followed by 30 min equilibration at this temperature.

^{32}P Labeling of oligonucleotides

The oligodeoxyribonucleotides were 5′-end labeled with ^{32}P using T4 polynucleotide kinase, [γ-^{32}P]ATP and standard procedure. Labeled RNAs were purified by 20% 7 M urea denaturing polyacrylamide denaturing gel electrophoresis (PAGE) and specific activities were measured using a Beckman LS 3801 counter.

Snake venom PDE ladder[15]

5′-[^{32}P]-labeled RNA (1.3 µM, specific activity 500000 cpm) were incubated with 200 ng of the phosphodiesterase I in a buffer, containing 50 mM tris–HCl (pH 8), 5 mM $MgCl_2$ at 21 °C. Total reaction volume was 50 µl. After 2, 10, 15, 30, 40 and 60 minutes aliquots (correspondingly 5, 6, 9, 9, 9 and 10 µl) were mixed with stop solution (correspondingly 10, 12, 18, 18, 18 and 20 µl), containing 0.05 M disodium salt of the ethylenediaminetetraacetic acid (EDTA), 0.05 % (w/v) bromophenol blue and 0.05% (w/v) xylene cyanole in 95% formamide. All aliquots were combined and subjected to 20% 7 M urea polyacrylamide denaturing gel electrophoresis and visualized by autoradiography.

Kinetics

(A) Calibration of RNase H concentration based on its cleavage activity. 15mer AON (**1**)–RNA (**3**) duplex: [AON] = 10^{-6} M, [RNA] = 10^{-7} M in a buffer, containing 20 mM tris–HCl (pH 8.0), 20 mM KCl, 10 mM $MgCl_2$, 0.1 mM EDTA and 0.1 mM dithiothreitol (DTT) at 21 °C in 30 µl of the total reaction volume has been used as a standard substrate to calibrate the amount of RNase H actually used. The percentage of RNA cleavage was monitored by gel electrophoreses as a function of time (2–5 min), with 0.06 U of RNase H, to give the initial velocity. *Thus, the initial velocity of the RNase H cleavage reaction (0.01208 µM min^{-1}) for the above standard substrate under the above condition corresponds to 0.06 units activity of enzyme in 30 µl of the total reaction mixture.* These are based on five independent experiments. Since the Michaelis–Menten equation, eqn. (1), suggests that the initial velocity of the reaction linearly depends upon the enzyme concentration, therefore, using the initial velocity of 0.01208 µM min^{-1} corresponding to 0.06 units/30 µl concentration of the RNase H, a correlation coefficient was found by dividing the observed experimental initial velocity by the standard initial velocity of 0.01208 µM min^{-1}. Then, the real enzyme concentration as well as the initial velocity in each experiment were corrected using this correlation coefficient, which was used to calibrate the initial velocity of the RNase H promoted cleavage reaction for each substrate presented in this work.

(B) AON concentration dependent experiments. AONs (0.01, 0.05, 0.1, 0.5 or 1 µM), with ^{32}P-labeled RNA (0.01 µM, specific activity 50000 cpm) were incubated with 0.06 units of RNase H in buffer, containing 20 mM tris–HCl (pH 8.0), 20 mM KCl, 10 mM $MgCl_2$, 0.1 mM EDTA and 0.1 mM dithiothreitol (DTT) at 21 °C. Total reaction volume was 30 µl. Prior to the addition of the enzyme reaction components were preannealed in the reaction buffer by heating at 80 °C for 5 min followed by 1.5 h equilibration at 21 °C. After 2–120 minutes, aliquots (3 µl) were mixed with stop solution (6 µl), containing 0.05 M disodium salt of the ethylenediaminetetraacetic acid (EDTA), 0.05 % (w/v) bromophenol blue and 0.05% (w/v) xylene cyanole in 95% formamide. This samples were subjected to 20% 7 M urea polyacrylamide denaturing gel electrophoresis and visualized by autoradiography. Quantitation of cleavage products was performed using a Molecular Dynamics PhosphorImager. The thermodynamic and kinetic parameters K_{d1} and V^{D}_{max} were obtained from v_0 *versus* $[D_0]$ = [AON] plots using eqn. (9). Values of K_{d1} and V^{D}_{max} were obtained by using the SigmaPlot 2000 Program, having the correlation equation: $y = ax/(b + x)$, where $x = [D_0]$, $a = V^{D}_{max}$ and $b = K_{d1}$.

(C) RNA concentration dependent experiments. ^{32}P-Labeled RNA (0.04, 0.06, 0.08, 0.1, 0.2, 0.4, 0.6 or 1 µM, specific activity 50000 cpm) with AONs (5 µM) were incubated with 0.06 units of RNase H in buffer, containing 20 mM tris–HCl (pH 8.0), 20 mM KCl, 10 mM $MgCl_2$, 0.1 mM EDTA and 0.1 mM dithiothreitol (DTT) at 21 °C. Total reaction volume was 30 µl. Prior to the addition of the enzyme, reaction components were preannealed in the reaction buffer by heating at 80 °C for 5 min followed by 1.5 h equilibration at 21 °C. After 3–10 minutes aliquots (3 µl) were mixed with stop solution (6 µl) and subjected to 20% 7 M urea denaturing gel electrophoresis. The kinetic parameters K_m and V_{max} were obtained from v_0 *versus* $[S_0]$ plots. Values of K_m and V_{max} from this method were determinated directly from v_0 *versus* $[S_0]$ plots by using of correlation SigmaPlot Program, where the correlation equation was: $y = ax/(b + x)$.

(D) Method for kinetic analysis. The kinetic analysis of RNase H promoted cleavage of the antisense-RNA duplex involves three distinct steps (see Fig 1): (i) the duplex formation (K_{d1}), (ii) the duplex (*i.e.* substrate)–enzyme complex formation (K_{d2}), and (iii) the cleavage of the substrate–enzyme complex (k_{cat}). Hence, at low substrate concentration, the Michaelis–Menten equation, eqn. (1), has been modified to eqn. (9) by combining eqn. (2) (dealing with initial velocity) and eqn. (8), which defines the state of the equilibrium constant of the duplex formation (K_{d1}), to address the influence of K_{d1}, K_{d2} and k_{cat} on the RNase H activity. Similarly at low substrate concentration, the extent of RNA cleavage, which is dependent on the K_{d1} value has been analyzed using eqn. (10), which is obtained by combining eqns. (5) and (8).

The Michaelis–Menten equation, eqn. (1),[16] as it stands, allows us to tackle the events only in steps (ii) and (iii).

$$v_0 = \frac{\Delta P}{\Delta t} = \frac{V_{max} S_0}{K_m + S_0} \quad (1)$$

Eqn. (1) can be used for monitoring RNA cleavage kinetics by RNase H only when RNA is saturated by AON, which is found in this work at 1–5 µM concentration of both the native and the oxetane-modified AONs. In this case, we can consider

that substrate concentration is equal to concentration of the RNA molecules.

Since we have used a wide range of AON and RNA concentrations in understanding the mechanism of RNA cleavage by RNase H under different substrate concentrations, we needed to modify the Michaelis–Menten equation, eqn. (1), both under low and high substrate concentration.

(A) Under *low substrate concentration*, when $S_0 \ll K_m$, eqn. (1) takes up the form of eqn. (2).

$$v_0 = \frac{V_{max}}{K_m} S_0 \tag{2}$$

This means that, when $S_0 \ll K_m$, v_0 is linearly dependent upon the substrate concentration with the linear coefficient of V_{max}/K_m.

(B) Under *high substrate concentration*, when $S_0 \gg K_m$, eqn. (1) can be rewritten as eqn. (3):

$$v_0 = V_{max} = k_{cat} E_0 \tag{3}$$

This means that v_0 in this case is dependent only on V_{max} or, alternatively, on k_{cat} and E_0.

The extent of the cleavage ($\alpha = [\Delta P]/S_0$) decreases inversely with an increase of substrate concentration, ($S_0 = [RNA]$), in accordance with the eqn. (4), which is a modified form of the Michaelis–Menten eqn. (1):

$$\alpha = \frac{\Delta P}{S_0} = \frac{V_{max} \Delta t}{(K_m + S_0)} \tag{4}$$

The eqn. (4) thus shows that under a low substrate concentration (S_0) (when $S_0 \ll K_m$), the extent of the cleavage α is not dependent upon the substrate concentration because when $S_0 \ll K_m$, eqn. (4) can be written as eqn. (5):

$$\alpha = \frac{\Delta P}{S_0} = \frac{V_{max}}{K_m} \Delta t \tag{5}$$

In this case, the extent of the cleavage is dependent only on the V_{max}/K_m ratio and the reaction time, Δt, and does not depend on substrate concentration, S_0.

However, when the substrate concentration is increasing, the extent of the cleavage decreases, and becomes close to zero in accordance with eqn. (4), and this dependence has hyperbolic shape. In high substrate concentration, when $S_0 \gg K_m$ eqn. (4) can be written as eqn. (4a):

$$\alpha = \frac{\Delta P}{S_0} = \frac{V_{max} \Delta t}{S_0} \tag{4a}$$

Under these conditions the extent of cleavage α depends on the V_{max} and substrate concentration, S_0 (eqn. (4)), and does not depend on K_m.

The effective turn over (N_{eff}) of RNase H per min can be calculated by using eqn. (6):

$$N_{eff} = \frac{\Delta P}{E_0} = \frac{S_0}{K_m + S_0} k_{cat} = F_e N_{max} \tag{6}$$

Where, N_{eff} indicates the number of RNA molecules (ΔP) the enzyme cleaves per min; F_e is the extent of enzyme (E) saturation by the substrate, S (or extent of enzyme–substrate complex, SE, formation), which is equal to zero, when $[S_0] = 0$, and equal to 1, when $[S_0] \gg K_m$ or $[S_0] \longrightarrow \infty$;

$$F_e = \frac{[SE]}{S_0} = \frac{S_0}{K_m + S_0} \tag{6a}$$

N_{max} is the maximal turn over of the enzyme per min, when the extent of saturation of the enzyme by substrate is maximal, otherwise when $F_e = 1$:

$$N_{max} = k_{cat} \tag{7}$$

Thus, eqn. (6) allows us to define N_{eff} at a definite substrate concentration, S_0, if we know the values for k_{cat} and K_m.

When an excess of [AON] towards [RNA] is used, the extent of saturation of RNA by AON, F_{RNA}, can be written however according to eqn. (8):

$$F_{RNA} = \frac{[DR]}{R_0} = \frac{D_0}{K_{d1} + D_0} \tag{8}$$

where DR is the AON–RNA hybrid duplex, D_0 is the initial AON concentration, R_0 is the initial RNA concentration and K_{d1} is equilibrium constant of dissociation of the hybrid AON–RNA.

In conditions where RNA is not saturated by AON and $S_0 \ll K_m$, eqn. (2) for initial velocity, v_0, or extent of cleavage α of reaction (eqn. (5)) can be rewritten as eqn. (9) or (10) by combining the formulae in eqns. (2), (5) and (8):

$$v_0 = \frac{V_{max}}{K_m} S_0 = \frac{V_{max}}{K_m} F_{RNA} R_0 = V^D_{max} F_{RNA} = \frac{V^D_{max} D_0}{K_{d1} + D_0} \tag{9}$$

$$\alpha = \frac{\Delta P}{R_0} = \frac{V_{max}}{K_m} F_{RNA} \Delta t \tag{10}$$

where V^D_{max} is the maximal initial velocity at saturation of RNA by AON (when $F_{RNA} = 1$), which equals:

$$V^D_{max} = V_{max} R_0 / K_m \tag{11}$$

Acknowledgements

Authors thank the Swedish Natural Science Research Council (NFR) and the Swedish Research Council for Engineering Sciences (TFR) and the foundation for Strategic Research (SSF) for generous financial support.

References

1 V. K. Rait and B. R. Shaw, *Antisense Nucleic Acid Drug Dev.*, 1999, **9**, 53.
2 B. R. Shaw, D. Sergueev, K. He, K. Porter, J. Summers, Z. Sergueeva and V. K. Rait, *Methods Enzymol.*, 2000, **313**, 226.
3 M. K. Ghosh, K. Ghosh and J. S. Cohen, *Anti-Cancer Drug Des.*, 1993, **8**, 15.
4 C. A. Stein, C. Subasinhghe, K. Shinozuka and J. S. Cohen, *Nucleic Acids Res.*, 1988, **16**, 3209.
5 M. Koziolkevich, A. Krakowiak, M. Kwinkowski, M. Boczkowska and W. J. Stec, *Nucleic Acids Res.*, 1995, **23**, 5000.
6 (*a*) S. Kanaya and M. Ikehara, *Subcell Biochem.*, 1995, **24**, 377–422; (*b*) I. Lebedeva and C. A. Stein, *Annu. Rev. Pharmacol. Toxicol.*, 2001, **41**, 403–419; (*c*) J. J. Toulme, P. Frank and R. J. Crouch, Human ribonuclease H, in *Ribonucleases H*, R. J. Crouch, ed., INSERM, Paris, 1998, ch. 7, pp. 147–162; (*d*) J. T. Miller, J. W. Rausch and S. F. Le Grice, *Methods Mol Biol.*, 2001, **160**, 335–354.
7 D. M. Tidd, *Perspectives Drug Discovery Des.*, 1996, **4**, 51.
8 (*a*) R. V. Giles and D. M. Tidd, *Anti-Cancer Drug Des.*, 1992, **7**, 37; (*b*) R. V. Giles and D. M. Tidd, *Nucleic Acids Res.*, 1992, **20**, 763.
9 D. M. Tidd, *Anticancer Res.*, 1990, **10**, 1169.

10 E. Kanaya and S. Kanaya, *Eur. J. Biochem.*, 1995, **231**, 557.
11 S. T. Crooke, K. M. Lemonidis, L. Neilson, R. Griffey, E. A. Lesnik and B. P. Monia, *Biochem. J.*, 1995, **312**, 599.
12 M. Haruki, Y. Tsunaka, M. Morikawa, S. Iwai and S. Kanaya, *Biochemistry*, 2000, **39**, 13939.
13 (*a*) S. Iwai, M. Wakasa, E. Ohtsuka, S. Kanaya, A. Kidera and H. Nakamura, *J. Mol. Biol.*, 1996, **263**, 699; (*b*) B. Verbeure, E. Lescrinier, J. Wang and P. Herdewijn, *Nucleic Acids Res.*, 2001, **29**, 4941.
14 (*a*) W. F. Lima and S. T. Crooke, *Biochemistry*, 1997, **36**, 390; (*b*) H. Wu, W. F. Lima and S. T. Crooke, *J. Biol. Chem.*, 1999, **274**(40), 28270.
15 N. V. Amirkhanov and J. Chattopadhyaya, *J. Chem. Soc., Perkin Trans. 2*, 2002, 271.
16 M. Dixon and E. C. Webb, in *Enzymes*, 3rd edn., Longman Group Ltd., London, 1979, p. 60.
17 A. Fersht, *Enzymatic Structure and Mechanism*, 2nd edn., Freeman, New York, 1985.
18 (*a*) M. J. Damha, C. J. Wilds, A. M. Noronha, I. Bruckner, G. Borkow, D. Arion and M. A. Parniak, *J. Am. Chem. Soc.*, 1998, **120**, 12976; (*b*) A. M. Noronha, C. J. Wilds, C. N. Lok, K. Viazovkina, D. Arion, M. A. Parniak and M. J. Damha, *Biochemistry*, 2000, **39**, 7050.
19 (*a*) J. Wengel, *Acc. Chem. Res.*, 1999, **32**, 301; (*b*) P. Herdewijn, *Biochim. Biophys. Acta*, 1999, **1489**, 167; (*c*) L. Kvaerno and J. Wengel, *Chem. Commun.*, 2001, 1419–1424.
20 (*a*) P. D. Cook, in *Antisense Research and Applications*, S. T. Crooke and B. Lebleu, eds., CRC Press Inc., Boca Raton, FL, 1993; (*b*) D. A. Braasch and D. R. Corey, *Chem. Biol.*, 2001, **8**, 1; (*c*) M. Manoharan, *Biochim. Biophys. Acta*, 1999, **1489**, 117; (*d*) K. H. Altmann, D. Fabbro, N. M. Dean, T. Geiger, B. P. Monia, M. Muller and P. Nicklin, *Biochem. Soc. Trans.*, 1996, **24**, 630; (*e*) E. Zamaratski, P. I. Pradeepkumar and J. Chattopadhyaya, *J. Biochem. Biophys. Methods*, 2001, **48**, 189–208.
21 (*a*) P. I. Pradeepkumar, E. Zamaratski, A. Földesi and J. Chattopadhyaya, *Tetrahedron Lett.*, 2000, **41**, 8601; (*b*) P. I. Pradeepkumar, E. Zamaratski, A. Földesi and J. Chattopadhyaya, *J. Chem. Soc., Perkin Trans. 2*, 2001, 402; (*c*) P. I. Pradeepkumar and J. Chattopadhyaya, *J. Chem. Soc., Perkin Trans. 2*, 2001, 2074.
22 P. Acharya, A. Trifonova, C. Thibaudeau, A. Foldesi and J. Chattopadhyaya, *Angew. Chem., Int. Ed.*, 1999, **38**, 3645.
23 (*a*) C. Thibaudeau and J. Chattopadhyaya, in *Stereoelectronic Effects in Nucleosides and Nucleotides and their Structural Implications*, Uppsala University Press, Uppsala, Sweden, 1999; (*b*) M. J. Frisch, G. W. Trucks, H. B. Schlegel, P. M. W. Gill, B. G. Johnson, M. A. Robb, J. R. Cheeseman, T. Keith, G. A. Petersson, J. A. Montgomery, K. Raghavachari, M. A. Al-Laham, V. G. Zakrzewski, J. V. Ortiz, J. B. Foresman, J. Cioslowski, B. B. Stefanov, A. Nanayakkara, M. Challacombe, C. Y. Peng, P. Y. Ayala, W. Chen, M. W. Wong, J. L. Andres, E. S. Replogle, R. Gomperts, R. L. Martin, D. J. Fox, J. S. Binkley, D. J. Defrees, J. Baker, J. P. Syewart, M. Head-Gordon, C. Gonzalez and J. A. Pople, Guassian 96 (Revision D.1), Guassian Inc., Pittsburgh, PA, 1995.
24 C. A. Stein, *J. Clin. Invest.*, 2001, **108**, 641.
25 C. Wahlestedt, L. Salmi, J. K. Good, T. Johnsen, T. Hokfelt, C. Broberger, F. Porreca, A. Koshkin, M. H. Jacobson and J. Wengel, *Proc. Natl. Acad. Sci. USA*, 2000, **97**, 5633.